Journal of the Meteorological Society of Japan, Vol. 88, No. 6, pp. 869–881, 2010.
DOI:10.2151/jmsj.2010-601

A GCM Study on Effects of Continental Drift on Tropical Climate at the Early and Late Cretaceous

Masamichi OHBA

Central Research Institute of Electric Power Industry, Chiba, Japan

and

Hiroaki UEDA

Graduate School of Life and Environmental Sciences, University of Tsukuba, Tuskuba, Japan

(Manuscript received 3 September 2008, in final form 8 June 2010)

Abstract

Simulations of the Early Cretaceous (120,000,000 years before the present day: 120 Ma) and the Last Cretaceous (65 Ma) have been performed using an atmospheric general circulation model (AGCM) coupled with a 1.5-layer reduced-gravity ocean model. After the initial spin-up period, both the runs are integrated for approximately 70 years. The simulation results confirm the occurrence of first-order changes in tropical atmospheric circulation in response to changes in the land/sea distribution. The simulation results show that the continental drift during the Cretaceous strongly affects the Walker and Hadley circulations. The birth of the Atlantic resulting from the breakup of the Gondwana continent causes splitting of a Walker circulation cell into two, and this in turn reduces the zonal gradient of the equatorial SST over the Pacific. The resultant SST warming in the equatorial Pacific enhances the Hadley circulation. The northward drift of the Indian continent causes significant SST warming in the Indian Ocean and intensifies the monsoon precipitation over Asia. It is also shown that the seasonal variations in the Asian monsoon are much stronger in the 65-Ma run than in the 120-Ma run. Interestingly, continental breakups cause the mega-monsoon system to split into distinct monsoon systems such as the Indian, South American, and African monsoon systems.

1. Introduction

The history of Earth's climate is largely based on the evidence from climate proxy data. These palaeoclimatic data indicate that the Cretaceous was one of the warmest periods in the Phanerozoic. The global annual mean surface temperatures were significantly higher than the present-day temperature (e.g., Barron 1983); this difference was attributed to the elevated atmospheric CO_2 levels in the Cretaceous (e.g., Berner 1990). It has also been established that the global sea levels for much of the Cretaceous were markedly higher than the present-day levels (e.g., Haq et al. 1987).

Recently, the atmospheric general circulation model (AGCM), the ocean general circulation model (OGCM), and the air-sea coupled general circulation model (CGCM) have been used to understand the Cretaceous climate. Numerical studies involving the use of these climate models have been performed to understand the Cretaceous climate and to demonstrate the importance of the geographical/continental distribution (Barron et al. 1993, 1995; Bush 1997; Otto-Bliesner and Upchurch 1997; Poulsen et al. 1999; Rees et al. 2000; Poulsen et al. 2001, 2003; Otto-Bliesner et al. 2002;

Corresponding author: Masamichi Ohba, Central Research Institute of Electric Power Industry (CRIEPI), Environmental Science Research Laboratory, 1646 Abiko, Abiko-shi, Chiba, 270-1194, Japan.
E-mail: oba-m@criepi.denken.or.jp

Donnadieu et al. 2006; Sellwood and Valdes 2006; Fluteau et al. 2007). In these studies, a combination of three major variables—continental distribution, atmospheric CO_2 level and oceanic heat flux—was used to determine the distribution of Cretaceous temperatures; among these variables, the latter two were considered the most important. Recent air-sea coupled model simulations of the Cretaceous also showed that the high atmospheric CO_2 levels in this period were responsible for the warmer climate and for the thermohaline circulation that was similar to the present-day case (Otto-Bliesner et al. 2002). Using the OGCM and CGCM, Poulsen et al. (1999, 2001, 2003) showed that palaeogeographic changes alter the oceanic circulation, leading to strong meridional overturning in the Atlantic Ocean and a subsequent reduction in the temperature gradient between the equator and the pole.

Numerous climate simulations have been carried out for the warm Cretaceous period, and climate models have been used for this purpose. Earth's surface has undergone considerable changes because of successive episodes of formation of continental landmasses via Wilson cycles, which resulted in the formation of supercontinents such as Pangea in the Phanerozoic (Wilson 1966). By using oceanic magnetic anomalies and palaeomagnetic data, we could reconstruct the paleo continental distribution until the Late Jurassic. The continental drift could explain the global and local climate changes. The latitudinal drift was found to have a notable effect on temperature because of the change in the incoming solar radiation level. Actually, the dispersal and formation of megacontinents such as Pangea during the Late Palaeozoic strongly affected the atmospheric circulation and climate (e.g., Kutzbach and Gallimore 1989). Hence, the mean global climate system was confirmed to be sensitive to plate motions, even if only the continental distribution underwent a change.

The previous studies mentioned above mainly focused on the response of the global climate to tectonic changes and to CO_2 caused by the global meridional atmospheric (e.g., Donnadieu et al. 2006) and oceanic (e.g., Poulsen et al. 2003) circulations and biogeochemical cycles (Misumi et al. 2009). In most of the previous experiments, the impact of major plate reorganization on the continental- and basin-scale climate that characterizes the Cretaceous, i.e., the break up of Gondwana and the northward shift of the Indian continent, was not accounted for. The influence of plate motions on the climate varies with the continental configuration. While knowledge of the location of a given continent is not sufficient for explaining global warm epochs, the role of the land/sea distribution becomes more significant in continental- and basin-scale atmospheric circulation.

The aim of this study is to gain a better understanding of how the paleo continental configuration in the Cretaceous affects the atmospheric circulation, especially over the tropics. The results of this study demonstrate that the changes occurring in the global atmospheric circulation in response to tectonic forcing are of the first-order. Although the model does not take into account biological or geochemical changes, it can simulate large-scale changes in the global atmospheric circulation, which may or may not be consistent with the proxies. The goal of our study is not to perform a realistic simulation of the climate evolutions during the Cretaceous by taking into account topographic boundary forcing (mountain height) and greenhouse gas effects but to perform different experiments by making changes to the continental configuration study, so that the effect of tectonic forcing on the tropical climate system during the Cretaceous becomes clear. In this study, the sensitivity of the tropical climate to changes in the major tectonic factors during the Cretaceous is examined to understand how atmospheric circulations respond to these environmental changes. Therefore, we attempt to simulate large-scale tropical circulations such as the Hadley, Walker, and monsoon circulations, which are the strongest driving forces of the general circulation at low latitudes. Two time slices, the Aptian (120 Ma) and the Maastrichtian (65 Ma), are analyzed because they have sufficiently different and interesting boundary conditions. The rest of this paper is organized as follows. Section 2 presents a brief description of the model used. Section 3 presents the simulated Cretaceous climate in the tropics. Section 4 presents the conclusions of the study.

2. Model

The present study focuses on the impact of plate motions on the climate in the Early and Late Cretaceous periods. The AGCM coupled with a 1.5-layer reduced-gravity ocean model is used for the experiments. The obtained results are expected to be relatively similar to those for fully coupled model simulations of the tropics. Two geological periods in the Cretaceous are selected: the Aptian (120 Ma) and

the Maastrichtian (65 Ma). These periods are characterized by the breakup of the Gondwana and the northward shift of the Indian continent.

We use the atmospheric component of the air-sea coupled model developed at the Meteorological Research Institute, Japan (MRI-CGCM2.3; Yukimoto et al. 2001; Yukimoto et al. 2006), for climate forecasting and paleo climate simulations (Kitoh et al. 2001; Kitoh and Murakami 2002). We employ a version with triangular truncation at zonal wave number 42 (T42) and a 30-layer hybrid sigma-pressure coordinate system. The nonlinear terms and parameterized physical processes are calculated using a 128×64 Gaussian grid with a horizontal resolution of about $2.8^\circ \times 2.8^\circ$. For further details of the model, readers are requested to refer to Shibata et al. (1999).

A 1.5-layer reduced-gravity linear ocean model (Zebiak and Cane 1987) is coupled with the atmospheric model in order to calculate the sea surface temperature (SST) at the surface boundary of the AGCM. This linear ocean model can be used for a crude representation of the seasonal heat capacity of the ocean mixed layer. The model grid has a horizontal resolution of 1° longitude $\times 0.5^\circ$ latitude. The SST is expressed as the mixed-layer temperature and is estimated on the basis of the balance between the surface heat fluxes, horizontal advection due to imposed winds, horizontal diffusion, and entrainment from below the slab mixed layer. In this model, the seawater temperature anomaly below the mixed layer (hereafter referred to as the subsurface temperature) is estimated on the basis of the thermocline depth anomaly. The slab mixed layer depth employed is 50 m, and the thermocline depth is 150 m.

The solar luminosity and Earth's orbital parameters are set to the present-day values; further, the concentrations of atmospheric trace gases, including methane and nitrous oxide, are also set to the present-day values. This experimental set up is similar to that reported by Ramstein et al. (1997). In the absence of global data for the Cretaceous, the major type of the vegetation is considered to be grasslands. All simulations are commenced from the zonal mean state. The initial atmospheric and oceanic temperatures are uniform in space.

The two different Cretaceous climates for the 120-Ma and 65-Ma runs are simulated on the basis of the impact of land-sea distributions. For a simple and fair estimation of the effect of continental drift, the land elevation is set to 840 m, which is derived from the mean altitude of the present-day land. The CO_2 concentration for both periods is assumed to be 1260 ppm. The two experiments are integrated for 70 model years. The following results are derived from the monthly mean conditions in the model years 40 to 70.

The hybrid coupled GCM has been widely used for the simulation of the tropical air-sea coupled system, especially for the study of idealized continents (e.g., Xie and Saito 2001; Okajima et al. 2003) and global warming (e.g., Eichler et al. 2006). It should be noted that the model has certain limitations, because of which it cannot be used for accurate climate simulation. First, nonlinear advection terms cannot be considered in the linear ocean model. Second, the slab-mixed/thermocline depth and the values of the other parameters considered in the ocean model are estimated on the basis of the current climate conditions. Third, the hybrid coupled GCM reproduces a relatively weak equatorial cold tongue in the eastern Pacific. Fourth, this model cannot simulate changes in the global oceanic circulation that can affect the interactions between the tropical latitudes and the mid-latitudes through the meridional oceanic circulation. Fifth, the CO_2 levels considered in the experiments is the same for both periods and is lower than that estimated from the proxy data. Our study mainly focuses on the effect of the continental drift, and therefore the other potential forcing factors such as vegetation and CO_2 level should be neglected in the experiments.

Figure 1 shows the latitudinal distribution of the continental mass. The paleoshorelines are represented by bold solid lines, as shown in Figs. 1b, c. The total continental mass in the 65-Ma (dashed line) run is slightly higher than that in the 120-Ma (solid line) run. The increases (decreases) in the continental masses along the latitudinal band of 20°S (60°S) is mainly attributed to the northward shift of the Indian continent. The Tethys Ocean (around 0°N–30°N, 60°W–60°E in the 120-Ma run) closure caused by the proximity of the African and Eurasian continents is also seen at around 20°N.

3. Cretaceous climate

3.1 Effect of tectonic forcing on the annual mean climate

While the Eurasian and North American continents did not experience major drifts during the Cretaceous, the Gondwana continent began

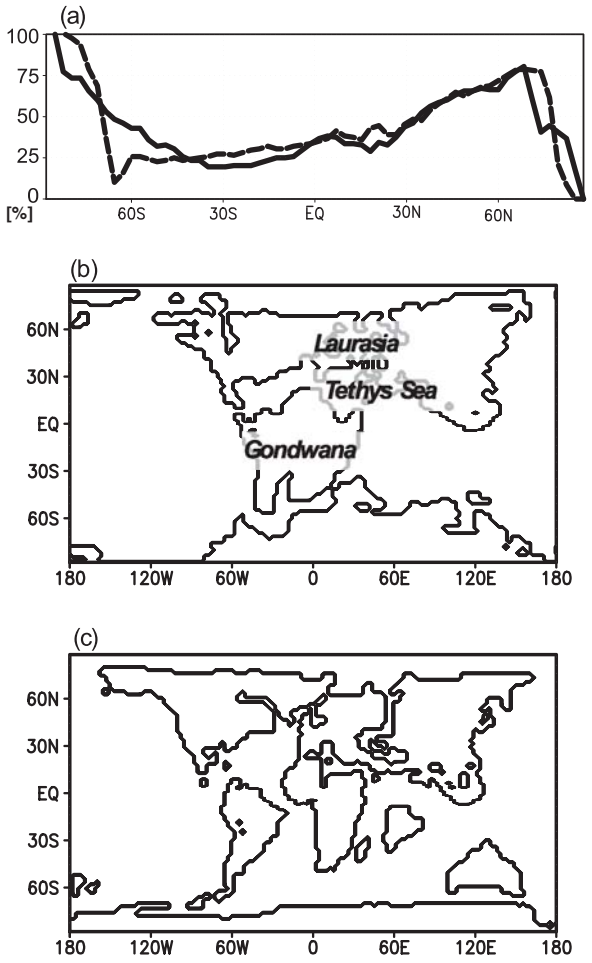

Fig. 1. (a) Latitudinal distribution of the percentage of continental mass along each longitudinal band in the 120-Ma run (solid line) and 65-Ma run (dash line). Land-sea distribution used in the AGCM for the (b) 120-Ma and (c) 65-Ma runs.

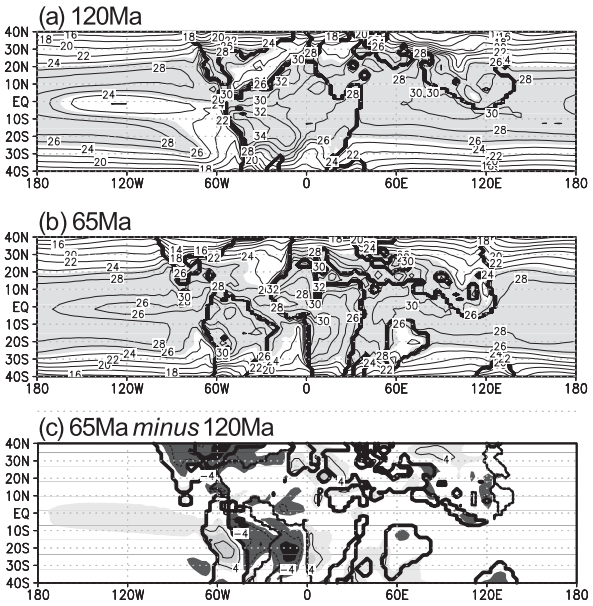

Fig. 2. Annual mean surface temperatures in the (a) 120-Ma and (b) 65-Ma runs. Light shaded areas indicate positive values greater than 25°C. (c) Difference in the abovementioned parameter between the 65-Ma and 120-Ma runs. The light (dark) shaded areas indicate positive (negative) values greater (lesser) than 2 (−2)°C. The area enclosed by the bold solid line (dash line) in (c) indicates a change from sea (land) to land (sea) via the continental drifts between 65 Ma and 120 Ma.

rifting apart since the Late Jurassic (Besse and Courtillot 1988). During the Aptian (125–112 Ma), the Gondwana continent was divided into three plates: Australia-Antarctica-India-Madagascar, South America, and Africa. This break up first began in the Australia-Antarctica-India-Madagascar continents, followed by the opening of the South Atlantic Ocean (around 30°W of the Southern Hemisphere, as shown in Fig. 1b). The Tethys Sea existed between the Gondwana continent (around 10°N–60°S, 60°W–40°E in the 120-Ma run) and the Laurasia continent (around 10–70°N, 70°W–130°E in the 120-Ma run) before the opening of the Atlantic Ocean. Its present remnants are the Black, Aral, and Caspian Seas. Because of the counterclockwise rotation of Africa and the westward drift of South America, maritime connection between the North and South Atlantic Ocean was well established by 65 Ma (around 70°S–40°N, 50°W–0°, as shown in Fig. 1c). The middle-to-late stages of the Cretaceous (90–65 Ma) were marked by the onset of rifting between Australia, India-Madagascar, and Antarctica. Finally, the Indian continent (around 20°S, 60°E, as shown in Fig. 1c) drifted away from Madagascar and began its rapid northward motion.

Figure 2 shows the annual mean distributions of the simulated surface temperature at the tropics in the 120-Ma run and 65-Ma run and the difference between the distributions in these runs. The simulated temperature distributions are relatively similar to those reported in a number of recent studies

(e.g., Otto-Bliesner et al. 2002; Sellwood and Valdes 2006; Donnadieu et al. 2006; Fluteau et al. 2007). The warmest temperature in the 120-Ma run is observed over the subtropics of the Gondwana continent at around 20°N/S (Fig. 2a). In the low-latitude areas, the annual temperature is relatively high, i.e., >25°C. Surface air temperatures of less than 20°C are observed over Siberia (around 30–40°N, 90°E) and southern Gondwana (around 30–40°S, 5°W–5°E). The continental regions between 20°N and 20°S are generally warm throughout the year and have sustained highs into the 30°C.

Comparison of the 120-Ma and 65-Ma runs clearly indicates that the continental break-up into South Atlantic, Africa, India, and Antarctica–Australia leads to fragmentation of the warmest areas into small regions (Fig. 2c). High surface temperatures of more than 30°C are found over the subtropics of the West Asian (around 20°N, 50°E), African (around 10°S, 0°), and South American continents (around 20°S, 60°W) (Fig. 2b). The birth of the Atlantic Ocean because of the plate movements of the continental areas across the Gondwana continent is a significant feature of the Late Cretaceous Earth. In response to the westward shift of the South American continent, the peak of the warm surface temperatures over the western Gondwana shifts from 40°W to 60°W at around 20°S. Moreover, warming of western Africa in relation to an enhanced subsidence and stability over the western coast of the continent (e.g., Shinoda and Kawamura 1996), which correspond to cooling of the surface temperature, are observed at 20°W. It is noted here that the Tethys Sea closure (around 10–20°N, 30°E, as shown in Fig. 2c) results in the formation of a warming region at around 10–30°N, 10–30°E. Because of the nature of our experimental setup, we assume that these environmental changes are mainly attributed to the changes in the *in situ* land/sea distributions (i.e., birth of the Atlantic Ocean).

Figures 3, 4 show the annual mean distributions of the SST, precipitation, and surface wind in the 120-Ma and 65-Ma runs, respectively. The simulated SST patterns for both periods well represent the general features that have already been observed in previous model studies (e.g., Bush 1997; Poulsen et al. 2001; Otto-Bliesner et al. 2002). The SST peak, which is recognized as a warm pool, exists in the tropical Indian Ocean (around 15°S–15°N, 30–120°E) in the 120-Ma run (Fig. 3a). The

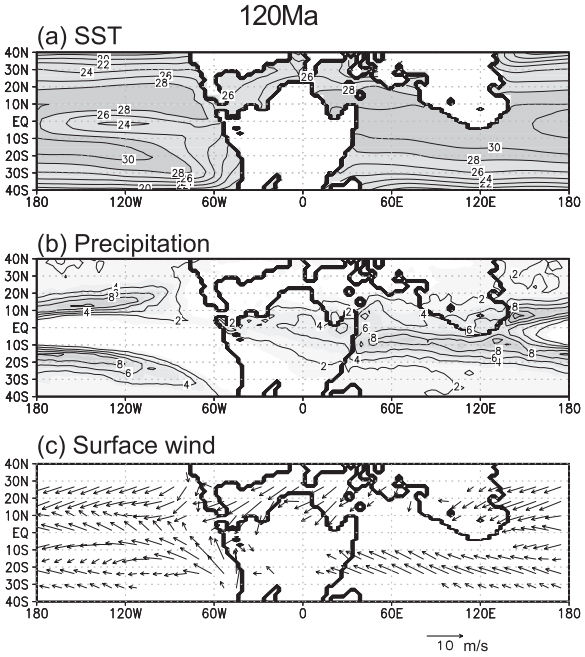

Fig. 3. Annual mean climates in the 120-Ma run in AGCM-simulated (a) SST (°C), (b) precipitation (mm/day), and (c) surface winds (m/s). Surface wind speeds that are lesser than 2 m/s are masked out.

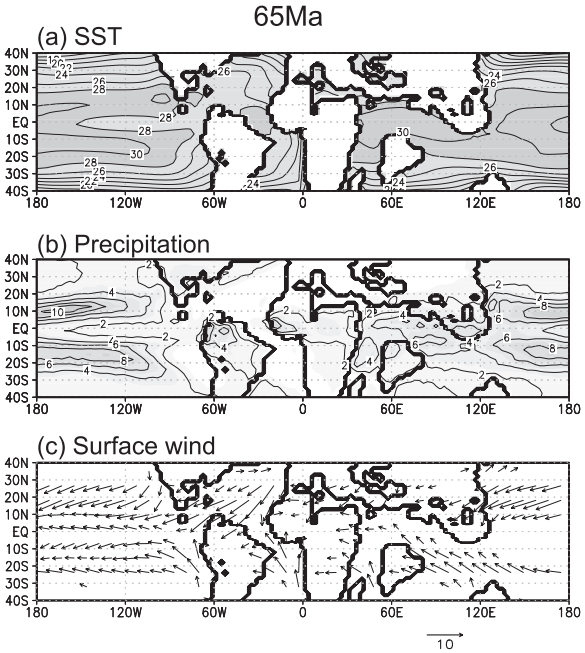

Fig. 4. Data shown are the same as in Fig. 3 but correspond to the 65-Ma run.

warm pool region experiences strong precipitation, and simultaneously, a strong equatorial easterly is observed over the tropical Pacific.'' (around 20°S–20°N, 120°E–60°W; Figs. 3b, c). The easterly trade wind is predominant over the tropical oceans except the northern Indian Ocean (40–80°E, eq-15°N) and causes a decrease in the SST through enhanced coastal upwelling and evaporative cooling. The equatorial easterly over the Pacific dominates the cool SST in the eastern part of the equatorial region, which is known as the cold tongue in the present-day climate. The simulated zonal gradient of the SST over the equatorial Pacific is consistent with that in Bush (1997), while the gradient is slightly stronger (by approximately 1°C).

The overall features of the SST pattern in the 65-Ma run are relatively similar to those of the present-day climate, although the simulated zonal gradient of the SST (2°C) in the equatorial Pacific is slightly weaker (Fig. 4a). The simulated SST of the tropical Indian Ocean as well as that of the tropical western-central Pacific (120–170°E) are also well above 30°C. The simulated tropical Pacific resembles the present-day El Niño/Southern Oscillation (ENSO)-like system, while the interannual variations are beyond the scope of this study.

The strong annual mean precipitations (>4 mm/day) are collocated with the high-SST region (i.e., region where the SST is greater than 28°C). Much of the tropical rainfall is recognizable over the oceans, with the main rainfall zone migrating north and south through the year in response to the movement of the intertropical convergence zone (ITCZ). Large precipitations are found over the equatorial Indian Ocean (40–80°E, 10°S–10°N), to the east of the equatorial Gondwana and off-equatorial Pacific in the 120-Ma run (Fig. 3b). The western tracts of Gondwana between 20°S and 40°S are simulated to receive very little rainfall. The tropical lands surrounding the eastern and central Tethys and the North Atlantic are also simulated to receive relatively little rainfall.

The birth of the Atlantic Ocean (30–40°W) causes significant changes in the world's rainfall patterns (Figs. 3, 4). Enhanced precipitation over the Amazonian watershed is seen in the northern part of South America (around 50°W, 10°S) in the 65-Ma run (Fig. 4b). The ITCZ, which stretches southeastward from the equator toward the southern Atlantic Ocean, is relatively similar to our well-known climate. The northward shift of the Indian continent, which is recognized to be an additional important continental change, weakens the strong precipitation (exceeding 8 mm/day) at the tropical Indian Ocean (60–120°E) in the 120-Ma run. The continental drift can also contribute to a distinct amplitude and phase modulation of the Cretaceous-Asian monsoon activity. The change in the annual mean precipitation can be attributed to the changes in the monsoon rainfall. This aspect will be discussed in the next sub section.

The most recent studies (e.g., Puceat et al. 2007), in which the oxygen isotope content of fossil fish teeth was used, show that the low-to-mid-latitude SST gradients in the Cretaceous are very similar to the present-day gradients. The results obtained by Amiot et al. (2004) are very similar to those reported by Puceat et al. (2007), although the reconstructed temperatures in the study conducte by Amiot et al. are the mean air temperatures in coastal lowlands. The results obtained by Amiot et al. (2004) and Puceat et al. (2007) indicate that the Cretaceous climate can be explained even if there are no drastic changes in the meridional oceanic heat transport. The meridional SST gradient in our model experiments is as strong as that in the present-day climate (Figs. 3a, 4a), similar to the case of previous model studies (e.g., Bush 1997; Poulsen et al. 2001; Otto-Bliesner et al. 2002).

The meridional atmospheric circulation in the tropics, known as the Hadley circulation, efficiently carries heat poleward and smoothes out horizontal temperature gradients. The equatorward motion near the surface is deflected westward, thus generating trade winds. Subsidence in the subtropics results in the formation of warm and dry desert regions through adiabatic descent air (Rodwell and Hoskins 1996). Many of the desert regions around the globe coincide with the sinking branch of the Hadley circulation. The Hadley and Walker circulations are determined to illustrate the difference between the wind fields in the tropics and the subtropics. In Figs. 5, 6, we show the mean meridional and zonal circulation. The definition of the Hadley and Walker circulation is same as that used by Kitoh and Murakami (2002). The Hadley circulation is determined by integrating the zonal mean meridional wind from the top of the atmosphere to the Earth surface. Similarly, the Walker circulation is determined by integrating the zonal wind between 30°S and 30°N.

Figure 5 shows the annual mean Hadley circulation for the 120-Ma and 65-Ma runs. The tropical

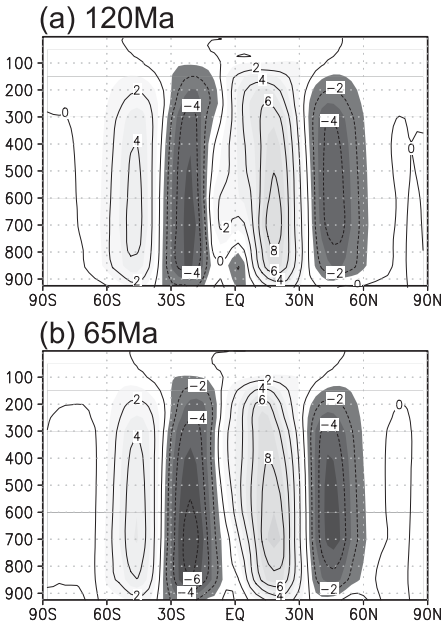

Fig. 5. Annual mean Hadley circulation for the (a) 120-Ma and (b) 65-Ma runs. The contour interval is 10^{10} kg/s. A positive value indicates a clockwise circulation in the diagram. Light (dark) shaded areas indicate positive (negative) values greater (lesser) than 1 $(-1) \times 10^{10}$ kg/s.

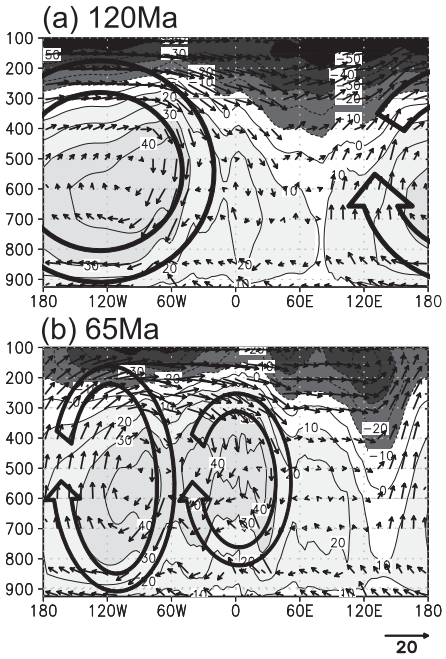

Fig. 6. Annual mean Walker circulation between 30°S and 30°N for the (a) 120-Ma and (b) 65-Ma runs. The contour interval is 10×10^{10} kg/s. A positive value indicates a clockwise circulation. The white-outlined arrows represent the Walker circulation cells.

Hadley cells in the 65-Ma run are slightly stronger than those in the 120-Ma run. In the early summer, the strength of the Southern Hemisphere tropical Hadley cell in the 65-Ma run is slightly stronger (about 30%) than that in the 120-Ma run (not shown). This result can be attributed to the increased continental masses at low latitudes or to the warmer conditions in the equatorial Eastern Pacific.

The Walker circulation is the zonal circulation over the tropical Pacific. Warm moist air embedded in the trade winds moves westward from the western coast of South America. The features of the tropical circulation in the 120-Ma run are related to those of a Walker circulation cell (Fig. 6a). In the annual mean, the strong Walker circulation over the Pacific results in the generation of equatorial upwelling Kelvin waves, which in turn can result in the shallowing of the thermocline in the eastern Pacific (not shown) and subsequent cooling (Fig. 3a). The annual mean Walker circulation in the 65-Ma run (Fig. 6b) is significantly different from that in the 120-Ma run. After the continental drift, the Walker circulation cell splits into two, as is evident from the surface wind (Fig. 4c). A slight weakening of the Walker cell is also evident over the central-eastern Pacific.

The results presented here correspond to the enhanced precipitation over the equatorial eastern Pacific and are consistent with the enhancement of the Hadley circulation in the 65-Ma run. The Walker circulation shows a strong annual cycle in the 120-Ma run but not in the 65-Ma run. Owing to the continental break up, which results in a more complex land/sea distribution, the global monsoon system is divided into distinct monsoon systems. The reduced amplitude of the annual cycle in the 65-Ma run may be attributed to changes in the global monsoon distribution. The analysis presented in the next section is focused on the seasonality of the precipitation, which affects global circulation.

3.2 Effect of tectonic forcing on the monsoon rainfall

Herein, we focus on the global monsoon, which is the dominant mode of annual variation in global

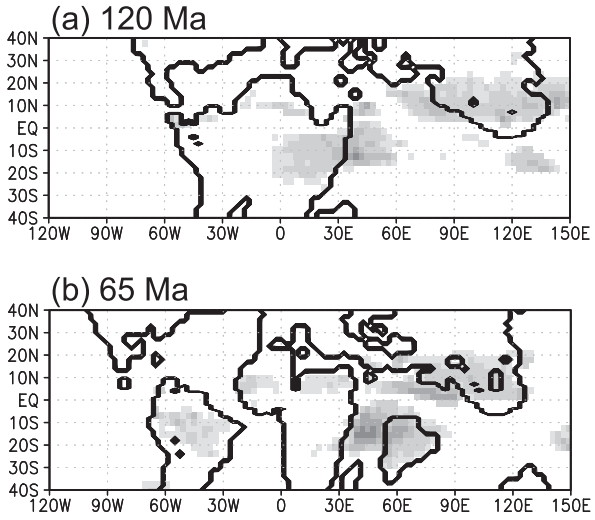

Fig. 7. Difference in the simulated precipitation between JJA and DJF. Shaded areas indicate absolute values of annual difference that are greater than 4 mm/day.

precipitation and circulation in response to changes in the annual insolation. The term ''monsoon'' is generally defined by the annual reversal of wind direction between winter and summer. However, examination of a time series of 850-hPa winds reveals that wind direction is not always a proper indicator of climate signals. Murakami and Matsumoto (1994) showed that for the definition of ''monsoon,'' distinct alternation of wet and dry seasons must be considered. Therefore, we identify the global monsoon region on the basis of the simulated seasonal mean precipitation. The definition of global monsoon in the present study calls for the occurrence of a well-defined wet climate during summer. Figure 7 shows the paleo global monsoon region defined by the difference in the precipitation between JJA (June, July, and August) and DJF (December, January, and February), which exceeds 4 mm/day. According to the aforementioned criterion, in the simulated 120-Ma, monsoonal climate is observed over the southern part of Eurasia and the eastern part of the Gondwana continent (Fig. 7a). The distribution of the monsoon regions changes significantly with the continental drift. In the early-to-late Cretaceous, the birth of the Southern Atlantic (around eq-40°S, 30°W) introduces a new South American monsoon around the present-day Rio Amazonas (eq-30°S, 30–60°W in Fig. 7b). The northward drift of the Indian continent also causes the center of the monsoon region to shift eastward from the eastern Gondwana to the Indian continent, suggesting that the Indian summer monsoon has already been established in the 65-Ma run.

Monsoon is driven by the thermal contrast between a relatively cool ocean and a warmer continent. While there are no mountains in the model, a thermal land/sea contrast does exist. The land/sea distributions play an essential role in monsoon evolution as well as in global climate changes. The advection of wet air masses by the low-pressure cell over the flat continent in summer has an important effect: release of latent heat due to moisture condensation and heavy precipitation over the southern or eastern edge of the continent. The model produces South Asian (around 90°E, 10°N) summer monsoon and East Asian (around 120°E, 10°N) summer monsoon as a result of the meridional temperature gradient over South Asia and the northward extension of the Asian summer monsoon rainbelt.

Figures 8, 9 show the seasonal mean precipitation and vertically integrated moisture flux on the boreal winter (DJF) and summer (JJA) for 120-Ma and 65-Ma runs, respectively. Additionally the difference between the abovementioned parameters in the 65-Ma and 120-Ma runs is shown in Fig. 10, for a more conclusive evidence of the effect of continental drift. The simulated mean seasonal precipitation in both periods corresponds to that in the simulations conducted by Sellwood and Valdes (2006).

In the 120-Ma run, significant precipitation is observed during the boreal summer over the northern Indian Ocean (Fig. 8c). South Asia and East Asia (around 90°E, 10°N) also experience strong precipitation, with moisture transport from the tropical Indian Ocean during the summer (Fig. 8d). The western and central parts of Eurasia are simulated to be almost dry throughout the year. In the Southern Hemisphere, a broad zone with strong precipitation extends from the equator to beyond 30°S in the boreal winter (Fig. 8a), embracing the western parts of Gondwana. In contrast, most of Gondwana remains dry in JJA (Fig. 8c).

However, after the breakup of Gondwana, the precipitation over the continent increases, especially in the tropical region (Figs. 9a, c). In the 65-Ma run, the northwestern part of South America is found to experience strong precipitation year-round, with moisture transport from the Atlantic,

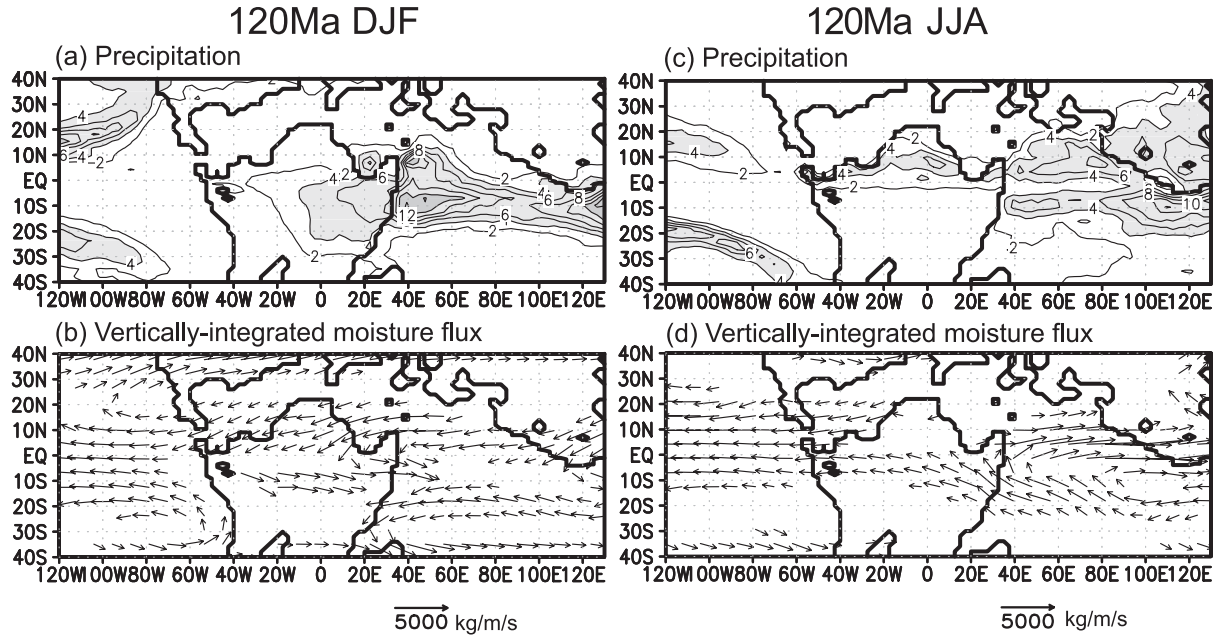

Fig. 8. (a) Precipitation and (b) vertically integrated moisture flux for the 120-Ma run during DJF. (c) and (d) are same as (a) and (b) but correspond to JJA. Moisture fluxes of less than 1000 kg/m/s are masked out.

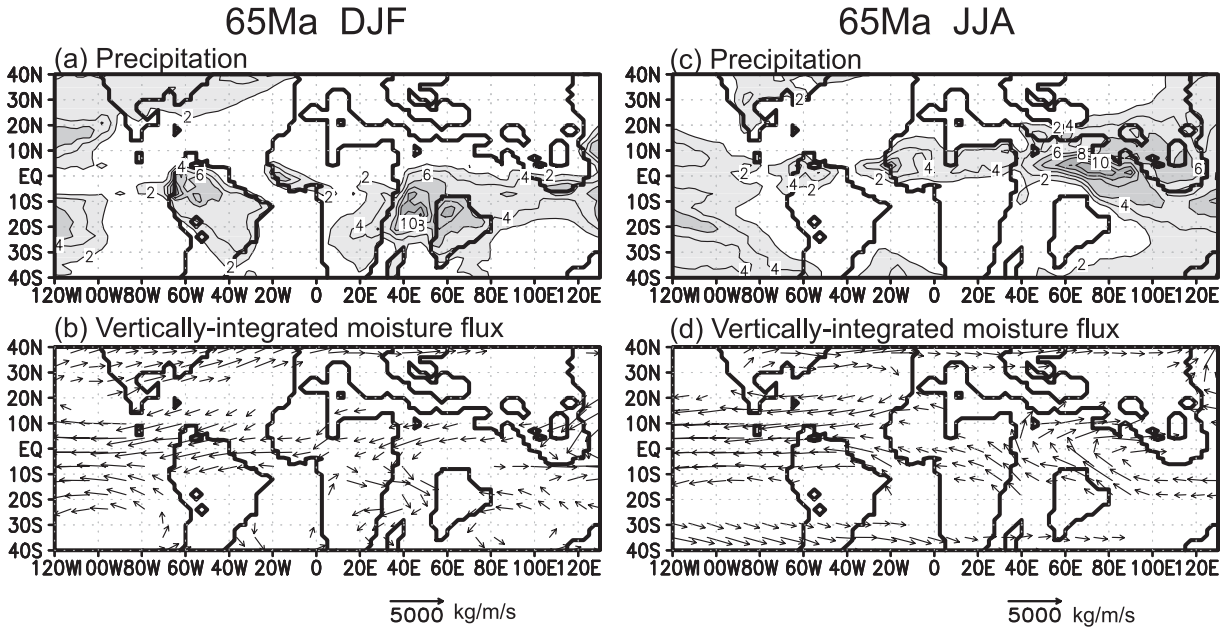

Fig. 9. Data are same as those in Fig. 8 but correspond to the 65-Ma run.

and hence, a tropical humid climate is expected. Similar to the 120-Ma run, Southeast Asia is predominantly humid with strong precipitation in JJA (Fig. 9c). The Indian continent located centrally in the Indian Ocean also experiences strong precipitation in the boreal winter (Fig. 9a).

As presented in the previous section, continental drift provides recasting of the global climate infor-

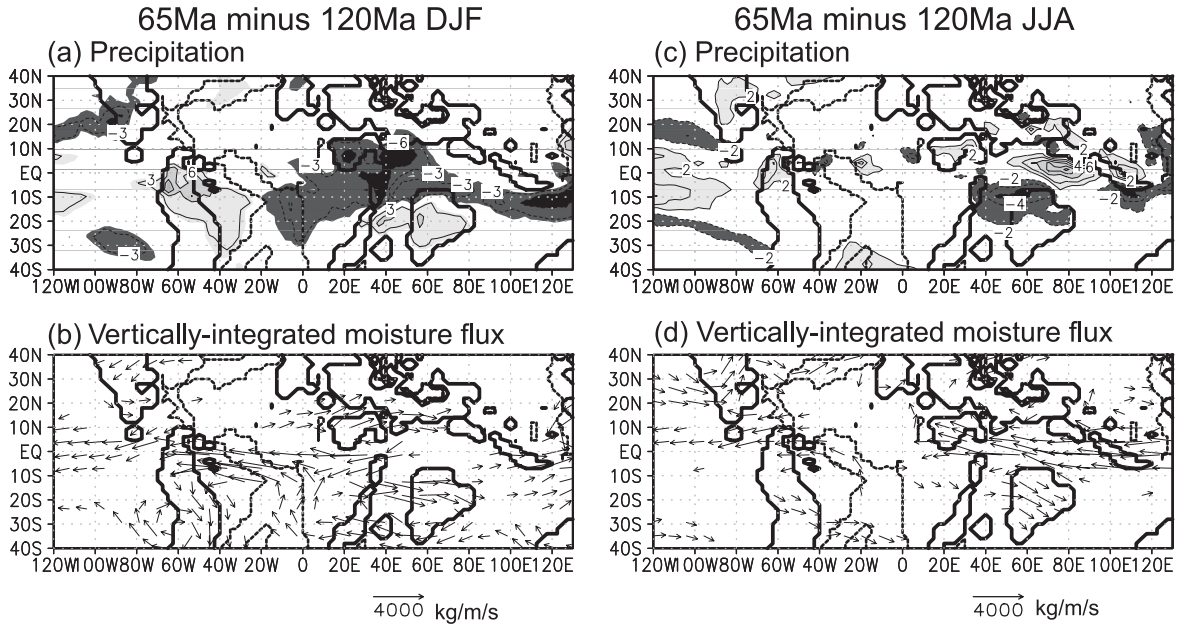

Fig. 10. Difference between the precipitation and vertically integrated moisture fluxes in the 65-Ma and 120-Ma runs. The bold solid line (dash line) denotes an increase (decrease) in the continental mass. The area surrounded by the bold solid line (dash line) indicates a change from sea (land) to land (sea) via continental drifts between 65 Ma and 120 Ma. Moisture flux vectors smaller than 800 kg/m/s are masked out.

mation. The northern parts of the South American and African continents (Gondwana) are simulated to have a monsoonal climate (Figs. 7a, b), with major rains commencing in the boreal winter (Fig. 9a). The difference between the precipitation and vertically integrated moisture flux in the 65-Ma and 120-Ma runs (Fig. 10) sheds light on the impact of continental drift on the monsoon system. After the birth of the Southern Atlantic, the precipitation around the present-day Rio Amazonas is enhanced in DJF (Fig. 10c). In contrast, reduced precipitation is found over the northern part of the African continent and the Tethys Sea in DJF. The changes in the simulated precipitation in JJA are distinctly different from those in DJF. Increased precipitation is observed along the coast of the southern parts of Eurasia and the equatorial Indian Ocean, suggesting that the intensity of the Asian summer monsoon is enhanced. This can be attributed not only to the change in the SST but also to the moisture convergence resulting from the modulation of global circulation. Interestingly, this feature is similar to those in future warm-climate simulations (Ueda et al. 2006). With the westward retreat of the coastline, the precipitation over southeastern Asia is reduced (100°E–120°E, 10°S–20°N). In the present-day climate, the precipitation in this region is strongly related to the effect of solar radiation (Ueda et al. 2009), implicating that a decrease in the landmass can directly affect the local precipitation.

Changes in the moisture flux in DJF (Fig. 10b) indicate a dramatic intensification of the easterly flux extending from the equatorial South American continent to the east coast of the African continent. The enhanced southeasterly moisture fluxes from the South Atlantic to the northern part of the South American continent supply moisture, which can result in precipitation enhancement. The northward shift of the Indian continent increases the austral summer precipitation across the continent (Fig. 10a). This enhanced precipitation is accompanied by an eastward moisture flux anomaly along 20°S, which is similar to the well-known feature of the Asian summer monsoon in the present-day climate. The generation of continental mass over the Southern Indian Ocean induces a slight southward shift of the ITCZ in the austral summer, and this results in reduced precipitation over the equatorial region. In addition, a northward shift of the Indian Ocean ITCZ by about 10° is seen in the boreal summer (Fig. 10c). Therefore, the seasonal meridional mi-

gration of the ITCZ is amplified in response to the northward shift of the Indian continent. This result implies that continental forcing can contribute significantly to the formation of the ITCZ (Xie and Saito 2001).

4. Concluding remarks

Most previous studies on the Cretaceous climate have focused on the relative impact of palaeogeography, ocean heat transport, and atmospheric CO_2 level. In this study, we selected two different geological periods corresponding to the start (120 Ma) and end (65 Ma) of the Cretaceous; these two periods differ considerably in their continental configuration. We simulated the 120-Ma and 65-Ma climate by using an AGCM coupled with a simple ocean model. The features of the simulated Cretaceous climate are similar to those reported in previous studies, such as surface temperature, precipitation, and SST (e.g., Bush 1997; Poulsen et al. 2001; Otto-Bliesner et al. 2002; Sellwood and Valdes 2006; Donnadieu et al. 2006; Fluteau et al. 2007); however, the simulated climate features provide deeper insights into the climate variations during the Cretaceous periods. Through sensitivity experiments, we investigated the role of palaeogeographic changes on the tropical climate, including the birth of the Atlantic Ocean and the northward shift of the Indian continent. There exists a significant difference between the climate in the 120-Ma and 65-Ma runs when there are changes in the land/sea distribution. Plate movements affect not only the local circulation but also the global circulation via modulation of the tropical Hadley and Walker circulation, which in turn is due to precipitation changes.

The birth of the South Atlantic Ocean introduces a new upward branch of the Walker circulation over the equatorial Southern America; consequently, the circulation cell is split into two. Because of the reduced Walker circulation over the tropical Pacific, the equatorial zonal gradient of the SST in the equatorial Pacific can be damped, which in turn may result in enhancement of the Hadley circulation. We also highlighted the changes in the global monsoon climate. Our model simulations of the Cretaceous shed light on the changes in the monsoon climate under different continental distributions. The continental break up makes more comprehensible maps about the monsoon climate. The birth of the Atlantic Ocean causes moisture convergence over the northern part of South America, and consequently, a new South American monsoon is established over the continent. It is also noted that the northward drift of the Indian continent enhances the summer and winter monsoon around South Asia (around 90°E, 10°N).

The originality of this study is that it involves the use of a hybrid coupled GCM for evaluating the effect of continental drift on the atmospheric circulation during the Cretaceous. Our sensitivity experiments are expected to be of help in understanding how tectonic forcing affects the tropical climate system during the Cretaceous. We focus on the relevant mechanisms rather than on detailed past climate trajectory. Many previous studies have used the AGCM coupled with a mixed layer model. The results of this study imply that simulation of the zonal gradient of the equatorial SST is important to understand the modulation of the Hadley circulation in the Cretaceous.

Using the AGCM coupled with the ocean mixed layer model, Fluteau et al. (2007) showed that the continental drift between the Cenomanian (around 95 Ma) and the Aptian resulted in reduced Asian monsoon precipitation in JJA. In contrast, the results of our experiments show enhanced precipitation over South Asia in the 65-Ma run. In the 65-Ma run, the Indian Ocean SST increases with the northward shift of the Indian continent. The enhanced precipitation is probably because the higher Indian Ocean SST in the 65 Ma. More detailed continental drift experiments must be performed to confirm this hypothesis.

Although our model is not perfect, the difference between the 65-Ma and 120-Ma periods based on the difference in the land/sea distributions can partly clarify the effect of continental drift on the tropical climate. While most previous studies on Cretaceous simulations focused on oceanic circulation (e.g., Poulsen et al. 2003), the present study focuses on the atmospheric circulation associated with the monsoon and involves the use of an air-sea coupled model. However, since there are very few atmospheric studies involving the use of proxy data (Hasegawa et al. 2009), we could not obtain proxy data on the monsoon precipitation or monsoon intensity in this period. In future, we plan to make up for the lack of proxy data by making use of a more realistic topography that includes mountains and carry out an interdisciplinary study based on a combination of atmospheric science and paleoclimatology. We believe that the results of the present study can be used to obtain a new proxy dataset that can help confirm our hypothesis. This

may facilitate fruitful discussions concerning the atmospheric general circulation system during the Cretaceous.

In future experiments, we plan to improve the boundary conditions (land-sea distributions at 120 Ma and 65 Ma without mountains) by using more realistic topographic conditions and a CGCM. We also plan to simulate the climate with the gradual continental distribution in order to give an explicit representation of the relationship between the geographical conditions and the climate changes occurring during the Cretaceous. Plans are underway for carrying out experiments on the accelerated continental drift, by using a model that considers only the birth of the Atlantic Ocean or the northward continental drift.

Acknowledgement

This research was supported by Grants-in-Aid for Young Scientists (B) (15740288) from the Japanese Ministry of Education, Science, Sports and Culture and Core Research for Evolutional Science and Technology (JST/CREST) and the Global Environment Research Fund (S-5-2) of the Ministry of the Environment, Japan. We thank Drs. A. Kitoh, S. Yukimoto, S. Murakami and O. Arakawa in MRI for valuable discussions and for providing the source code of MRI-CGCM. We express our special thanks to Drs. K. Misumi of the Central Research Institute of Electric Power Industry (CRIEPI) and M. Abe of the National Institute for Environmental Studies (NIES) for helpful discussions. We also acknowledge the valuable comments of two reviewers.

References

Amiot, R., C. Lécuyer, E. Buffetaut, F. Fluteau, S. Legendre, and F. Martineau, 2004: Latitudinal temperature gradient during the Cretaceous, Upper Campanian–Middle Maastrichtian: ∂18O record of continental vertebrates, *Earth and Planetary Science Letters*, **226**, 255–272.

Barron, E. J., 1983: A warm, equable Cretaceous: the nature of the problem. *Earth Sci. Rev.*, **19**, 305–38.

Barron, E. J., W. H. Peterson, D. Pollard, and S. L. Thompson, 1993: Past climate and the role of the oceanic heat transport: model simulations for the Cretaceous. *Paleoceonography*, **8**, 785–798.

Berner, R. A., 1990: GEOCARB II: A revised model of atmospheric CO_2 over Phanerozoic time, *Am. J. Sci.*, **301**, 182–204.

Besse, J., and V. Courtillot, 1988: Paleogeographic maps of the continents bordering the Indian Ocean since the Early Jurassic. *J. Geophys. Res.* **93**, 11791–11808.

Bush, A. B. G., 1997: Numerical simulation of the Cretaceous Tethys Circumglobal Current. *Science*, **275**, 807–810.

Donnadieu, Y., R. Pierrehumbert, R. Jacob, and F. Fluteau, 2006: Modelling the primary control of paleogeography on Cretaceous climate, *Earth and Planetary Science Letters*, **248**, 426–437.

Eichler, T., D. Rind, and S. Zebiak, 2006: Impact of Global Warming on ENSO Variability Using the Coupled GISS GCM/ZC Model. *Intl. J. Climatology*, **26**, 1283–1314.

Fluteau, F., G. Ramstein, J. Jean Besse, R. Guiraud, and J. P. Masse, 2007: Impacts of palaeogeography and sea level changes on Mid-Cretaceous climate. *Palaeogeography Palaeoclimatology Palaeoecology*, **247**, 357–381.

Haq, B. U., J. Hardenbol, and P. R. Vail, 1987: Chronology of fluctuating sea levels since the Triassic, *Science*, **235**, 1156–1167.

Hasegawa, H., R. Tada, X. Jiang, Y. Suganuma, S. Imsamut, P. Charusiri, N. Ichinnorov, and Y. Khand, 2009: Drastic shrinking of the Hadley circulation during the mid-Cretaceous Supergreenhouse, Submitted to *Geology*.

Kitoh, A., S. Murakami, and H. Koide, 2001: A simulation of the Last Glacial Maximum with a coupled atmosphere-ocean GCM. *Geophys. Res. Lett.*, **28**, 2221–2224.

Kitoh, A., and S. Murakami, 2002: Tropical Pacific climate at the Mid-Holocene and the Last Glacial Maximum simulated by a coupled ocean-atmosphere GCM. *Paleoceanography*, **17(3)**, 1047, doi:10.1029/2001PA000724.

Kutzbach, J. E., and R. G. Gallimore, 1989: Pangaean climates: megamonsoons on the megacontinent. *J. Geophys. Res.*, **94 (D3)**, 3341–3357.

Misumi, K., Y. Yamanaka, and E. Tajika, 2009: Numerical simulation of atmospheric and oceanic biogeochemical cycles to an episodic CO_2 release event: implications for the cause of mid-Cretaceous Ocean Anoxic Event-1a, *Earth Planet. Sci. Lett.* **286**, 316–323.

Murakami, T., and J. Matsumoto, 1994: Summer monsoon over the Asian continent and western North Pacific. *J. Meteor. Soc. Japan*, **72**, 719–745.

Okajima, H., S.-P. Xie, and A. Numaguti, 2003: Interhemispheric coherence of tropical climate variability: Effect of climatological ITCZ. *J. Meteor. Soc. Japan*, **81**, 1371–1386.

Otto-Bliesner, B. L., and G. R. Upchurch Jr., 1997: Vegetation-induced warming of high-latitude regions during the Late Cretaceous period. *Nature*, **385**, 804–807.

Otto-Bliesner, B. L., E. C. Brady, and C. Shields, 2002: Late Cretaceous ocean: coupled simulations with

the National Center for Atmospheric Research Climate System Model. *J. Geophys. Res*, **107 (D2)**, 4019–4029. doi:10.1029/2001JD000821.

Poulsen, C. J., E. J. Barron, C. C. Johnson, and P. Fawcett, 1999: Links between major climatic factors and regional oceanic circulation in the mid-Cretaceous. In: Barrera, E., Johnson, C. C. (Eds.), Evolution of the Cretaceous ocean-climate system. *Geol. Soc. Am.*, **332**, 73–89.

Poulsen, C. J., E. J. Barron, M. A. Arthur, and W. H. Peterson, 2001: Response of the mid-Cretaceous global oceanic circulation to tectonic and CO_2 forcings. *Paleoceanography*, **16 (6)**, 574–590. doi:10.1029/2000PA000579.

Poulsen, C. J., A. S. Gendaszek, and R. L. Jacob, 2003: Did the rifting of the Atlantic Ocean cause the Cretaceous thermal maximum? *Geology*, **31**, 115–118.

Puceat, E., C. Lecuyer, Y. Donnadieu, P. Naveau, H. Cappetta, G. Ramstein, B. T. Huber, and J. Kriwet, 2007: Fish tooth delta 180 revising late cretaceous meridional upper ocean water temperature gradients, *Geology*, **35**, 107–110.

Ramstein, G., F. Flteau, J. Besse, and S. Joussaume, 1997: Effect of orogeny, plate motion and land-sea distribution on Eurasian climate change over the past 30 million years. *Nature*, **386**, 788–795.

Rees, P. M., A. M. Ziegler, and P. J. Valdes, 2000: Jurassic phytogeography and climates: new data and model comparisons, in Huber, B. T., Macleod, K. G., and Wing, S. L., eds., *Warm climates in Earth history: Cambridge, Cambridge University Press*, 297–318.

Rodwell, M. J., and B. J. Hoskins, 1996: Monsoons and the dynamics of deserts. *Quart. J. Roy. Meteor. Soc.*, **122**, 1385–1404.

Sellwood, B. W., and P. J. Valdes, 2006: Mesozoic climates: General circulation models and the rock record. *Sedimentary Geology*, **190**, 269–287.

Shibata, K., H. Yoshimura, M. Ohizumi, M. Hosaka, and M. Sugi, 1999: A Simulation of Troposphere, Stratosphere, and Mesosphere with an MRI/JMA98 GCM, *Pep. in Meteo. and Geophys.*, **50**, 15–53.

Shinoda, M., and R. Kawamura, 1996: Relationships between rainfall over semi-arid southern Africa, geopotential heights, and sea surface temperatures. *J. Meteor. Soc. Japan*, **74**, 21–36.

Ueda, H., A. Iwai, K. Kuwako, and M. E. Hori, 2006: Impact of anthropogenic forcing on the Asian summer monsoon as simulated by 8 GCMs. *Geophs. Res. Lett*, **33**, L06703, doi:10.1029/2005GL025336.

Ueda, H. M. Ohba, and S.-P. Xie, 2009: Important factors for the development of the Asian-Northwest Pacific summer monsoon. *J. Climate*, **22**, 649–669.

Wilson, J. T., 1966: Did the Atlantic close and then reopen? *Nature*, **211**, 676–681.

Xie, S.-P., and K. Saito, 2001: Formation and variability of a northerly ITCZ in a hybrid coupled AGCM: Continental forcing and ocean-atmospheric feedback. *J. Climate*, **14**, 1262–1276.

Yukimoto, S., A. Noda, A. Kitoh, M. Sugi, Y. Kitamura, M. Hosaka, K. Shibata, S. Maeda, and T. Uchiyama, 2001: The New Meteorological Research Institute Coupled GCM (MRI-CGCM2)—Model Climate and Variability, *Pap. Meteorol. Geophys.*, **51**, 47–88.

Yukimoto, S., A. Noda, A. Kitoh, M. Hosaka, H. Yoshimura, T. Uchiyama, K. Shibata, O. Arakawa, and S. Kusunoki, 2006: Present-Day Climate and Climate Sensitivity in the Meteorological Research Institute Coupled GCM Version 2.3 (MRI-CGCM2.3). *J. Meteor. Soc. Japan*, **84**, 333–363.

Zebiak, S. E., and M. A. Cane, 1987: A model El Niño Southern Oscillation. *Mon. Wea. Rev.*, **115**, 2262–2278.